

Rapid Entrainment-Forced Freshening of the Iceland Scotland Overflow

Manish Devana¹, William E. Johns², Sijia ZOU³, and Adam Houk⁴

¹University of Miami, Rosenstiel School of Marine and Atmospheric Sciences

²Rosenstiel School of Marine and Atmospheric Science, University of Miami

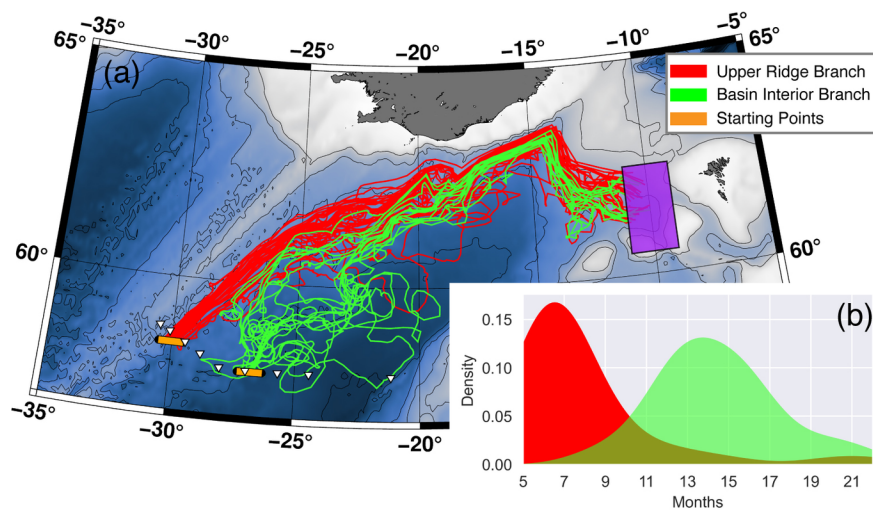
³Duke University

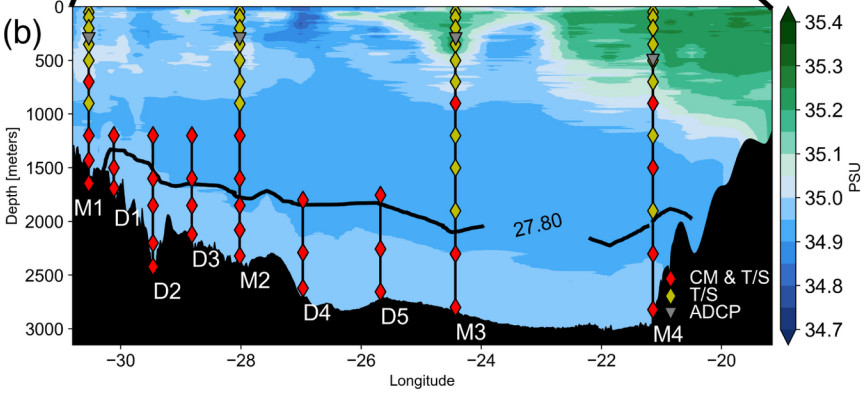
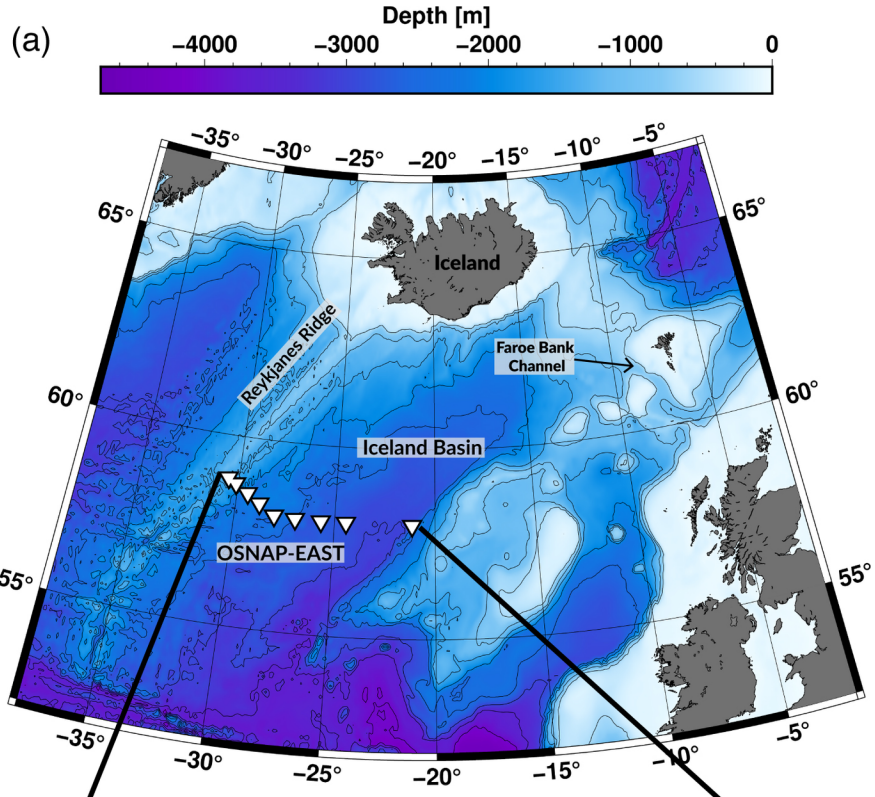
⁴University of Miami

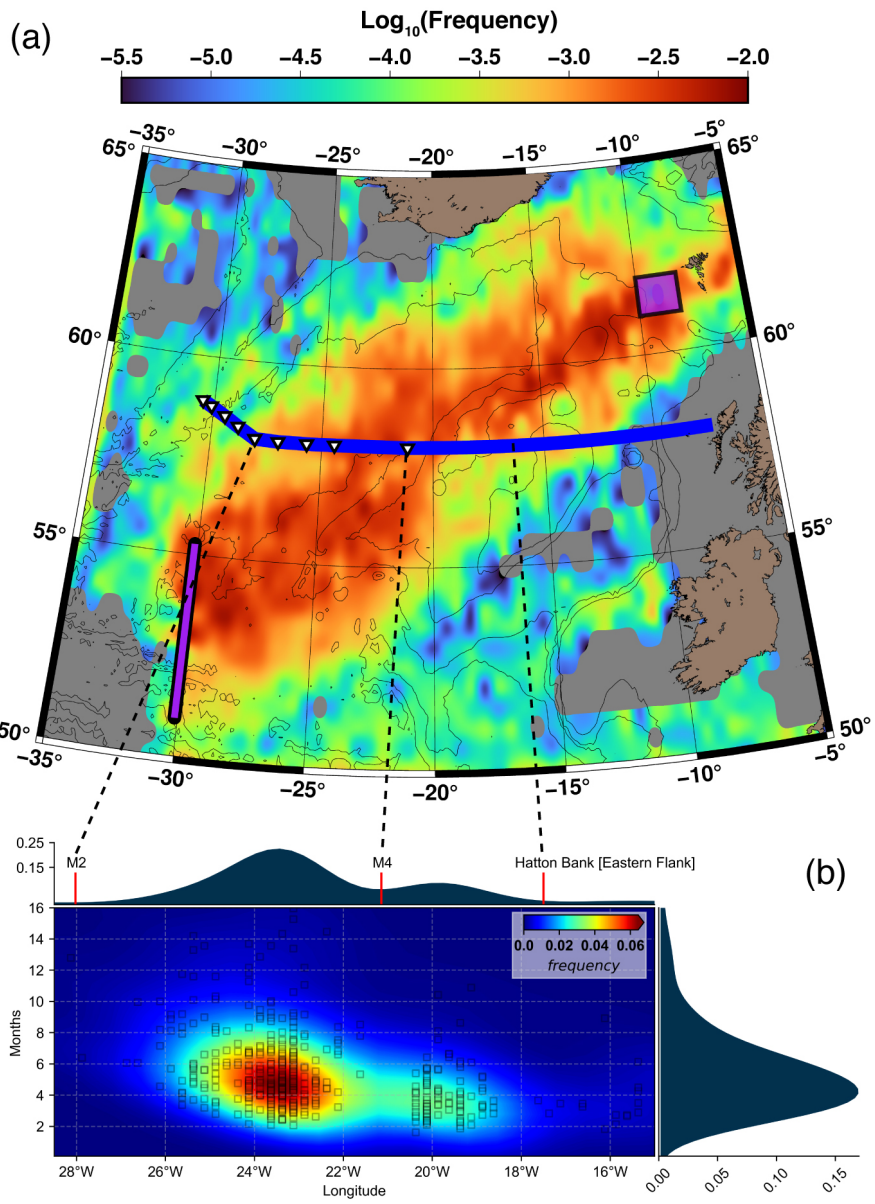
November 28, 2022

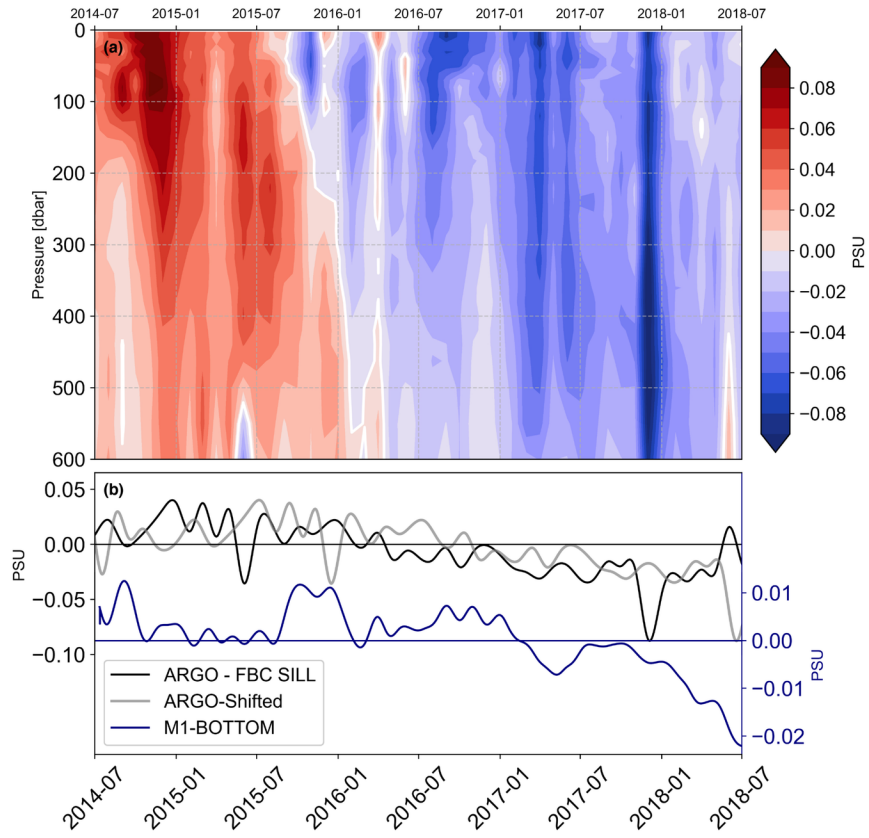
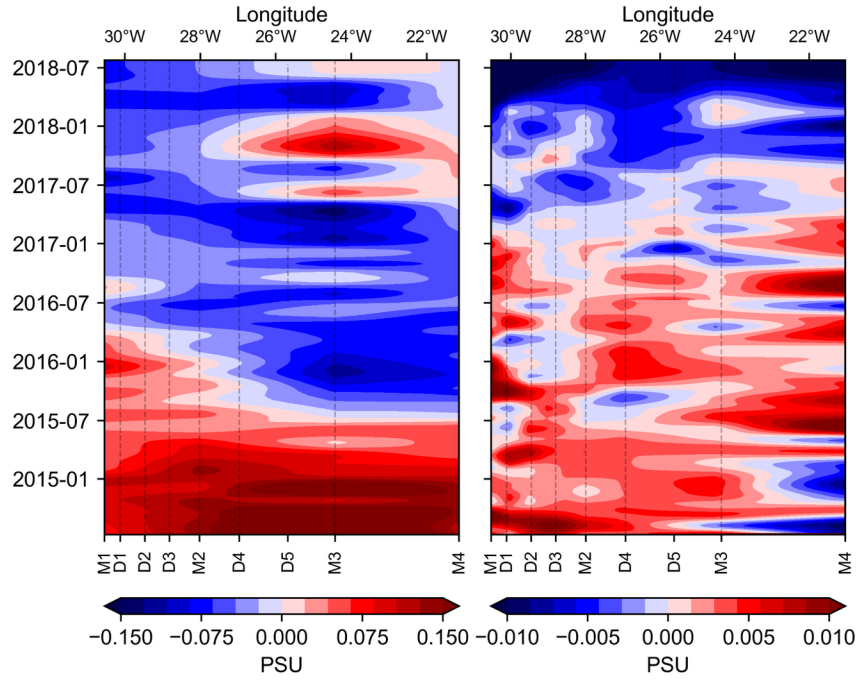
Abstract

Newly available mooring observations from the Overturning in the Subpolar North Atlantic Program (OSNAP) show an abrupt decline in Iceland Scotland Overflow (ISOW) salinity from 2017 to 2018 summer. Previous declines in ISOW salinity of similar magnitude have largely been attributed to changes in convectively formed deep waters in the Nordic seas on decadal time scales. We show that this rapid decline in salinity was driven by entrainment of a major upper ocean salinity anomaly in the Iceland Basin. This is shown by tracking the propagation of the upper ocean anomaly into ISOW using a combination of mooring and Argo observations, surface drifter trajectories, and numerical model results. A 2-year total transit time from the upper ocean into the ISOW layer was found. The results show that entrainment allows for rapid modification of ISOW, and consequently the lower limb of Atlantic Meridional Overturning Circulation, on sub-decadal timescales.









Rapid Entrainment-Forced Freshening of the Iceland Scotland Overflow

Manish S. Devana¹, William E. Johns¹, Adam Houk¹, Sijia Zou²

¹Rosenstiel School of Marine and Atmospheric Sciences, University of Miami

²Woods Hole Oceanographic Institute

Key Points:

- Significant freshening of the Iceland Scotland Overflow plume is observed in the Iceland Basin
- Salinity changes in the overflow plume are directly linked to changes in the upper ocean through entrainment
- Entrainment significantly modifies North Atlantic deep water mass properties on sub-decadal timescales.

Abstract

Newly available mooring observations from the Overturning in the Subpolar North Atlantic Program (OSNAP) show an abrupt decline in Iceland Scotland Overflow (ISOW) salinity from 2017 to 2018 summer. Previous declines in ISOW salinity of similar magnitude have largely been attributed to changes in convectively formed deep waters in the Nordic seas on decadal time scales. We show that this rapid decline in salinity was driven by entrainment of a major upper ocean salinity anomaly in the Iceland Basin. This is shown by tracking the propagation of the upper ocean anomaly into ISOW using a combination of mooring and Argo observations, surface drifter trajectories, and numerical model results. A 2-year total transit time from the upper ocean into the ISOW layer was found. The results show that entrainment allows for rapid modification of ISOW, and consequently the lower limb of Atlantic Meridional Overturning Circulation, on sub-decadal timescales.

Plain Language Summary

New observations from the Overturning in the Subpolar North Atlantic Program (OSNAP) show a major decline of deep ocean salinity in a layer known as the Iceland Scotland Overflow (ISOW). The ISOW layer is an important component of the deep ocean circulation in the North Atlantic formed through a mixing of cold, deep water from the Nordic Seas and salty, mid-depth water in the Atlantic. Previously recorded salinity changes of similar magnitude in the ISOW layer have occurred over timescales greater than a decade. This ISOW freshening event is traced back to a major freshening of the upper ocean that propagated into the ISOW layer through entrainment, a process of intense mixing between deep and mid ocean waters. Using a combination of numerical model output, Argo and surface drifter data, and moored observations, we show that entrainment facilitated a significant change to the ISOW layer in just 2-3 years.

1 Introduction

Iceland Scotland Overflow Water (ISOW) is a major constituent of the Atlantic Meridional Overturning Circulation's southward, abyssal flow. ISOW is formed from warm, salty upper ocean waters delivered to the North Atlantic Subpolar Gyre and Nordic Seas via the North Atlantic Current (NAC) (Hansen & Østerhus, 2007). After its formation, ISOW is exported out of the Iceland Basin through gaps in the Mid Atlantic Ridge and mixes with other deep water masses to form North Atlantic Deep Water, the dominant southward flowing water mass in the AMOC. Understanding the drivers of variability in ISOW is therefore critical to understanding variability in the whole AMOC system.

Hydrographic variability within the abyssal ISOW layer is linked to its source water masses. Two distinct processes converge to form ISOW: convection in the Nordic Seas and entrainment along the Iceland Faroe Ridge (IFR). Convection transforms warm, salty upper ocean water into cold, dense, deep water in the Nordic seas, which then flows southwards across the IFR (Johns et al., 2021-Under Review; Hansen & Østerhus, 2007; Fogelqvist et al., 2003; García-Ibáñez et al., 2015). The majority of the Nordic Seas overflow crossing the IFR is funneled through the Faroe Bank Channel (FBC) before spilling into the Iceland Basin. Entrainment occurs as the flow spills out of FBC and descends into the abyssal layer as a gravity current (Hansen & Østerhus, 2000, 2007). This process mixes warm, salty upper ocean waters into the overflowing waters, creating the final ISOW water mass. Cumulatively across the entire IFR, the entrainment process nearly doubles the total transport from 3 Sv of the original Nordic Seas overflow crossing the IFR to 5.3 Sv (Johns et al., 2021-Under Review). The similar volumetric contributions of convectively formed deep water and entrained waters into the overflow implies that property variations in either the overflow waters or entrained waters can have a significant impact on the final ISOW properties.

Newly available mooring observations from the Overturning in the Subpolar North Atlantic (OSNAP) show major upper ocean subpolar gyre freshening, followed by an abrupt

65 decline in ISOW salinity 2 years later. The upper ocean freshening event was the most
66 intense salinity decline observed in 120 years and was driven by changes in subpolar gyre
67 circulation (Holliday et al., 2020). The OSNAP observations raise the question: Did the
68 upper ocean event force the ISOW freshening, and if so, through what mechanisms? We
69 demonstrate here the upper ocean’s ability to force substantial hydrographic variabil-
70 ity in ISOW on sub-decadal timescales through the entrainment pathway. The pathway
71 is defined as the upper ocean NAC and the abyssal ISOW layer flow connected by en-
72 trainment at Faroe Bank Channel.

73 Multiple upper ocean freshening events in the subpolar gyre have been documented
74 in the last 100 years. Previous efforts to track the propagation of these events show 3-
75 6 year upper ocean advection times from the gyre to the Nordic Seas (Belkin, 2004). How-
76 ever, the lack of abyssal layer observations prevented past studies from linking singular
77 upper ocean events to changes in abyssal waters such as ISOW. Dickson et al. (2002) showed
78 that a decadal scale decline of ISOW salinity in the 1990’s was due to widespread fresh-
79 ening in the regions of deep water formation north of the subpolar gyre. They suggest
80 that entrainment acted to reinforce changes already present in the convectively formed
81 overflow waters. However, the recently observed decline of salinity in the ISOW plume
82 occurred just 2 years after the upper ocean freshening event and was as large in mag-
83 nitude as the decade long decline described by Dickson et al. (2002). This strongly points
84 to entrainment as the mechanism responsible for the recent ISOW freshening.

85 To demonstrate that entrainment of the upper ocean salinity anomaly was the cause
86 of the ISOW freshening, we tracked the anomaly’s propagation along the expected en-
87 trainment pathway. A combination of Argo derived salinity fields, surface drifter tra-
88 jectories, and the FLAME (Family of Linked Atlantic Model Experiments) ocean model
89 are used for tracking the anomaly and investigating its pathway. Our methods are de-
90 tailed in the next section followed by the results along each segment of the entrainment
91 pathway, and concluding remarks on the implications of this study.

2 Data and Methods

2.1 OSNAP mooring array

The OSNAP mooring array crosses the entire North Atlantic subpolar gyre, capturing the upper and lower limbs of the AMOC (Lozier et al., 2019). Here we focus on the OSNAP-East section which crosses the Iceland Basin from the Reykyanes Ridge to the Hatton Bank (Fig. 1). The array provides hourly hydrographic measurements of the NAC and ISOW flows from July 2014 to July 2018. For a detailed description of the entire OSNAP array readers are referred to Lozier et al. (2019), and to Johns et al. (2021-Under Review) for further details on the OSNAP-East section. The eastern side of the array, mainly moorings M3 and M4, sample the northward flowing NAC waters while the western side captures the southward, bottom trapped ISOW (Fig. 1). For this study we utilize the instruments in the upper 300 meters of the mooring array to represent the near surface waters of the Iceland Basin, and the near-bottom instrument at each mooring to represent the ISOW properties. These measurements capture the salinity anomaly as it is advected across the OSNAP line but give no further details on the advective pathways through the basin. For this we turn to surface drifters, Argo derived hydrography, and results from a numerical model.

2.2 Surface Drifters and Super-trajectories

Surface drifter trajectories, at hourly resolution, from the AOML Global Surface Drifter Dataset are used to investigate the upper ocean connection of the NAC to the region of the FBC sill where entrainment occurs (Elipot et al., 2016). All trajectories from drogued in the Iceland Basin from 2005-2018 are used to construct a transit matrix for a $0.25^\circ \times 0.25^\circ$ grid of the eastern subpolar gyre. The transit matrix approximates the probability of a particle moving from any particular grid cell to any other cell over a fixed timescale (Ser-Giacomi et al., 2015; McAdam & Sebille, 2018).

117 Using the transit matrix, we simulate super-trajectories in a Markov Chain Monte
118 Carlo simulation that moves particles across the grid by using the probabilities contained
119 in the transit matrix (Seville et al., 2011; Ser-Giacomi et al., 2015). We simulate 10^4 tra-
120 jectories to thoroughly sample the distributions of drifter movements. Further detail on
121 the construction of the transit matrix and super-trajectories can be found in Support-
122 ing Information-S1.

123 Trajectories are initiated in the NAC upstream (south) of the OSNAP line before
124 the current turns northward and splits into several branches. From this set of trajecto-
125 ries, we focus the analysis on those which reach the "entrainment zone", a region imme-
126 diately downstream of the FBC sill (indicated in Fig. 3). By initializing the trajectories
127 upstream of the OSNAP line we can identify all the advective pathways connecting the
128 NAC to FBC and their associated timescales.

129 **2.3 Argo Climatology**

130 The Roemmich-Gilson Argo (RGA) monthly analysis is used to observe the time
131 evolution of salinity in upper ocean NAC waters downstream of FBC where the bulk of
132 entrainment occurs. The RGA analysis has a $1^\circ \times 1^\circ$ resolution and spans 2004-2018 (Roemmich
133 & Gilson, 2009). Using the grid point closest to the FBC (9.5°W , 61.5°N), a time se-
134 ries of salinity anomalies is constructed. The salinity anomalies are calculated relative
135 to the 2014-2018 mean, matching the period of the OSNAP records. The record is also
136 de-seasonalized to remove the effects of seasonal precipitation anomalies that impact the
137 upper ocean salinity across the entire subpolar region.

138 **2.4 FLAME model trajectories**

139 Output from the Family of Linked Atlantic Model Experiments (FLAME) is used
140 trace the flow in the ISOW layer southwards to the OSNAP line. These model simula-
141 tions were used as part of investigations into downstream ISOW pathways by Gary et
142 al. (2011); Zou et al. (2017). Drifters were released every 3 months from 1992 to 1994

143 at various depths within the ISOW layer (i.e at depths below the 27.8 kg/m^3 isopycnal)
144 in the two main branches of ISOW flow at the OSNAP line and their trajectories were
145 computed backwards in time for 24 months. The upper ridge branch and a basin inte-
146 rior branch were identified in the observational studies by Zou et al. (2017) and Johns
147 et al. (2021-Under Review). Although FLAME output does not span the OSNAP ob-
148 servational record, sensitivity experiments show that advective pathways are represen-
149 tative of typical ISOW flow and should not affect our major conclusions (Gary et al., 2011).

150 The trajectories are forced with the 3-D velocities at 3 day time steps, integrated
151 backwards in time until reaching the vicinity of the FBC sill. Only trajectories reach-
152 ing the FBC entrainment zone were included in the analysis. These trajectories provide
153 an estimate of the typical pathways and typical timescales of particles in the ISOW plume
154 that travel southward from the FBC to the OSNAP line.

155 **3 Results**

156 **3.1 OSNAP Observations**

157 The OSNAP array shows a major upper ocean decline in salinity beginning in July
158 2015 (Fig. 2a). Freshening occurs first on the eastern side of the array, in the NAC. Up-
159 per ocean salinity minima are observed in November 2015 and March 2017 at the loca-
160 tion of mooring M3. The magnitude of freshening varies over the time between these two
161 minima but the salinity anomaly remains negative through this period. Meanwhile on
162 the western side of the array, negative anomalies arrive in May 2016 and persist through
163 the end of the record. This is consistent with the freshening signal being advected around
164 the Iceland basin, following the cyclonic subpolar gyre circulation. The cause of this up-
165 per ocean salinity anomaly was shown by Holliday et al. (2020) to be linked to an anoma-
166 lous diversion of freshwater from the Labrador Shelf into the the NAC, combined with
167 wind driven circulation changes. We are focused on the propagation of this anomaly into
168 the ISOW layer. Salinities within the ISOW layer abruptly decline beginning in January

169 2017, first at M1 near the crest of the Reykjanes Ridge, followed by freshening eastward
170 across the basin. Negative anomalies spread eastward across the array, reaching D5 by
171 July 2017, near the eastern limit of the ISOW plume. After the initial arrival of the fresh-
172 ening pulse in March 2017, positive salinity anomalies occur at D2-D4 for a 2-3 month
173 period before resumption of an overall freshening trend. Salinities continually decrease
174 across the entire array through the end of the record with nearly all moorings showing
175 a greater than 0.01 PSU decline. We believe the freshening observed in the eastern Ice-
176 land Basin is related to the recirculation and mixing of ISOW into the region rather than
177 direct pathways from the FBC overflow to the eastern part of the basin (Johns et al.,
178 2021-Under Review). The overall 2 year decline in salinity of ISOW is comparable in mag-
179 nitude with the "Great Salinity Anomaly" decadal scale freshening event of the 1990's
180 documented by Dickson et al. (2002).

181 The OSNAP observations show a 1.5-2 year lag between upper ocean and overflow
182 layer freshening. If the upper ocean anomaly is forcing the ISOW changes, this lag pro-
183 vides an estimate of the advection time from the NAC entering the Iceland Basin to the
184 ISOW being exported southwards from the basin. Below we examine the advective path-
185 way in three stages: northward advection to Faroe Bank Channel, entrainment into the
186 overflow, and southward advection to the OSNAP line within the ISOW layer. By con-
187 structing a timeline of this pathway and comparing it with the estimated lag from the
188 OSNAP array we can verify that entrainment is responsible for the ISOW freshening.

189 **3.2 Advection within the NAC to Faroe Bank Channel**

190 The drifter derived super-trajectories show the advective pathway connecting the
191 North Atlantic Current to Faroe Bank Channel, the first limb of the entrainment path-
192 way. Figure 3 shows the frequency of super trajectory positions for trajectories that reach
193 the entrainment zone. The highest frequencies are seen following the eastern Iceland Basin
194 topography north eastwards towards the Faroes. This agrees well with the known paths
195 of the North Atlantic Current and the Hatton/Rockall Bank jets. The trajectory dis-

196 tributions also extend eastward towards the western side of the Rockall Trough but do
197 not indicate a significant pathway to the FBC directly through the Rockall Trough.

198 To further dissect the various branches associated with the NAC to FBC connec-
199 tion, we can examine the longitudinal distributions of the trajectories and the associated
200 advection times. The distribution of super-trajectories crossing 58°N shows two peaks,
201 a main peak centered near 24°W and a secondary peak near 20°W . The larger peak, ac-
202 counting for 65% of trajectories, crossing the OSNAP line between $26\text{--}22^{\circ}\text{W}$, indicates
203 that the NAC branch through the Iceland Basin delivers the bulk of upper ocean wa-
204 ters to the entrainment zone. Advection times from the OSNAP line to FBC in this branch
205 range between 2-8 months. The smaller peak, 20% of trajectories, indicates a narrow
206 branch of flow between $21\text{--}19^{\circ}\text{W}$ which advects waters to FBC within 2-4 months. This
207 narrow and faster branch occurs in the region of the Hatton Bank Jet, shown by Houpert
208 et al. (2018) to be a region of enhanced northward NAC flow trapped along the east-
209 ern slope of the basin. The super-trajectory results suggest that these two NAC branches
210 reaching FBC deliver 80% of particles in 2-8 months, with an average arrival time of
211 4.8 months.

212 **3.3 Entrainment into the Iceland Scotland Overflow**

213 The RGA reconstruction of salinity anomalies at FBC clearly shows the arrival of
214 the freshening signal and its downward propagation to entrainment depths. Figure 4 shows
215 the arrival of negative anomalies in the upper 300 meters in October 2015, 3 months af-
216 ter freshening at the OSNAP array. The timing of this freshening is consistent with the
217 shorter end of the advective timescales estimated from the super-trajectories. However,
218 the actual entrainment only occurs at depths of 600-800 meters, corresponding to the
219 depths of the overflow layer as it spills out of the FBC (Hansen & Østerhus, 2007). Through
220 winter and spring of 2016 the freshening signal propagates down to entrainment depths,
221 where it persists through the summer of 2018. The downward propagation of the salin-
222 ity anomaly is likely associated with Subpolar Mode Water formation, a seasonal pro-

223 cess occurring through much of the northern Iceland Basin (Brambilla & Talley, 2008;
224 Brambilla et al., 2008). The delayed arrival of negative salinity anomalies at depth could
225 also be partly due to slower subsurface advective speeds in the NAC compared to those
226 at the surface. The continuous negative salinity signal at depth shows that the overflow
227 was entraining anomalously fresh waters from spring 2016 through summer 2018. In com-
228 bination with the super trajectories, the Argo record shows that anomalies entering the
229 Iceland Basin in the NAC are entrained into the overflow approximately 6-12 months
230 after they are advected to FBC and mixed to sufficient depth.

231 **3.4 Southward Propagation in the Iceland Scotland Overflow Plume**

232 Once entrained, the upper ocean freshening signal propagates within the Iceland-
233 Scotland Overflow plume’s pathway along the eastern flank of Reykjanes Ridge. We cross-
234 correlated salinity anomaly records at every bottom mooring with the RGA time series
235 at 600 meters in Figure 4 to estimate the lag between salinity changes at FBC and in
236 the overflow layer at the OSNAP array. A maximum correlation is seen at M1 ($r=0.42$,
237 at $P<0.05$) with a 7-8 month lag. The bottom M1 record lies in upper part of the ISOW
238 layer, closest to the Reykjanes Ridge crest. Weaker correlations are also present with moor-
239 ing records to the east down the ridge slope with generally longer lags. This is consis-
240 tent with model-based evidence presented below that indicates longer and more circuitous
241 pathways of flow in the ISOW layer towards the Iceland Basin interior.

242 We applied an 8 month shift to the RGA salinity record at FBC for a closer com-
243 parison with the salinity record at M1 (Fig. 4). There is some variability in the appar-
244 ent arrival times of salinity anomalies in the ISOW plume, with the initial onset of the
245 freshening trend at M1 occurring in January 2017, about 10 months after it began at
246 the entrainment site, and the large freshening anomaly at the end of the M1 record, in
247 July 2018, appearing to occur about 7 months after the maximum freshening anomaly
248 at the entrainment site in November 2017. These variations can be explained in part by
249 the low temporal resolution of the RGA dataset as well as internal variability of the ISOW

250 plume. Combined with the upper ocean transit time to the entrainment zone, we esti-
251 mate an approximate total 1.5-2 year advection time from the NAC crossing the OSNAP
252 line in the upper ocean to ISOW being exported southward out of the basin. This fits
253 well with the lag observed in Figure 2, however the results also raise two key questions:
254 Is a 7-10 month lag consistent with the ISOW flow, and why does the freshening signal
255 take longer to arrive in the interior of the Iceland Basin?

256 **3.5 ISOW pathways in FLAME**

257 The FLAME model results display the variable ISOW flow pathways through the
258 Iceland Basin (Fig. 5). Backward pathways from the upper branch of the ISOW plume
259 to the FBC sill follow the topography of the Reykjanes Ridge and the Iceland Faroe Ridge.
260 The 5-9 month advection times in the upper branch agree well with the M1 cross-correlation
261 estimated times (Fig. 5; b-inset). Mooring records at several locations along the Reyk-
262 janes Ridge confirm a more laminar, consistently southward flow close to the ridge axis
263 (Kanzow & Zenk, 2014; Johns et al., 2021-Under Review). Basin interior branch trajec-
264 tories follow the Iceland Faroe Ridge and then detach from the topography as the flow
265 turns southward along the RR. The basin interior trajectories are longer and more cir-
266 cuitous than those in the upper branch. This results in longer, more variable advection
267 times of 12-18 months from FBC to the OSNAP array. The longer advection times found
268 in the basin interior branch of ISOW flow explain the delayed onset of freshening across
269 the ISOW layer (Fig. 2b). Onset of freshening on the eastern side of the basin (near M4)
270 is likely explained by horizontal mixing associated with energetic, quasi-isotropic vari-
271 ability in the central Iceland basin as well as sub-basin recirculation recirculations ev-
272 ident in the mooring array data (SI-S3).

273 The model results and the OSNAP records suggest that the advection time from
274 FBC out of the Iceland Basin ranges from 6 months near the Reykyanes Ridge to >15
275 months in the basin interior. Combined with the upper ocean advective timescales of

276 6-12 months, this shows that salinity anomalies in the upper ocean can modify the en-
277 tire ISOW layer in 1.5-2 years.

278 **3.6 Salinity Signal on the Convective Pathway**

279 Past studies of salinity anomalies in the ISOW layer show longer timescales of prop-
280 agation from the upper ocean into ISOW that are linked primarily with changes in the
281 convectively formed Norwegian Sea Overflow Waters. During the time period of this fresh-
282 ening event, mooring observations in the Norwegian Sea Overflow layer in the Faroe Bank
283 Channel, upstream of entrainment, show no significant, sustained, freshening signal as
284 of the most recent recovery of data from FBC in the summer of 2018 (Personal Com-
285 munication; B. Hansen 2019). Additionally, Argo observations in the Norwegian Sea do
286 not show the arrival of a freshening signal until January 2017 (SI, Fig. S3), and the sig-
287 nal fails to penetrate depths greater than 600 meters through the summer of 2018. Both
288 sets of observations show that overflow waters in the Nordic Seas have not yet been sig-
289 nificantly freshened to explain the observed freshening. The presence of fresher waters
290 in the upper ocean of the Norwegian Sea suggests that convectively formed deep waters
291 here may eventually carry the freshening signal to FBC. However, it is unclear if or when
292 that signal may appear clearly in the overflow waters. Complex deep Norwegian Basin
293 and Greenland Sea circulation and stabilizing effects of the deep water reservoir feed-
294 ing the overflows suggest that convection does not directly link the upper and deep flows
295 in the same manner as entrainment (Shao et al., 2019).

296 Finally, we consider whether the magnitude of the ISOW freshening signal is con-
297 sistent with the magnitude of the upper ocean freshening event, via the process of en-
298 trainment. Johns et al. (2021-Under Review) show the final ISOW product contains about
299 25% of entrained Subpolar Mode Water. If entrainment of the upper ocean anomaly is
300 the main cause of the $O(0.01)$ PSU ISOW freshening, this would imply a salinity decline
301 of 0.04 PSU in the Subpolar Mode Water that is entrained into the overflow. Figure 4
302 shows freshening on the order of 0.02-0.06 PSU at the level of entrainment into the over-

303 flow at the FBC, which is consistent with the above estimate. Therefore, the initial salin-
304 ity anomaly of the near-surface waters of the Iceland Basin of $O(0.1 \text{ PSU})$, after being
305 diluted by vertical mixing down to the level of entrainment at FBC (0.04 PSU), can ex-
306 plain the $O(0.01 \text{ PSU})$ freshening of the ISOW layer through entrainment of about a 1:4
307 volume ratio of SPMW into the final ISOW product watermass. If freshening of over-
308 flow waters does occur in the future while entrained waters remain anomalously fresh,
309 the ISOW freshening may be expected to increase in the next years to decade.

310 **4 Conclusions**

311 Our results demonstrate that the recently observed freshening in the Iceland Scot-
312 land Overflow waters was caused by entrainment of a major upper ocean salinity anomaly.
313 Upon entering the Iceland Basin, anomalously fresh waters took about to 6-8 months
314 to reach the entrainment zone near Faroe Bank Channel and propagate down to depths
315 of active entrainment. Once entrained, the salinity anomaly took 1-1.5 years to spread
316 southward in the ISOW layer back to the OSNAP line, leading to total advection time
317 of 1.5-2 years. The combined effects of entrainment and the associated currents allow
318 for rapid and significant modifications to ISOW and, consequently, North Atlantic Deep
319 Water salinity on a sub-decadal timescale. Previous studies have repeatedly highlighted
320 the AMOC's sensitivity to salinity changes (Josey et al., 2018; Hátún et al., 2005). Fu-
321 ture work from a more basin wide perspective can be used to investigate the downstream
322 North Atlantic Deep Water and AMOC response to this rapid ISOW salinity freshen-
323 ing event.

324 **Acknowledgments**

325 The authors would like to thank the captains and crews of the R/V Knorr, R/V Pela-
326 gia, RRS Discovery, and R/V Neil Armstrong, as well as the University of Miami Ocean
327 Technology Group, for their able assistance in the seagoing operations supporting this
328 research. Financial support for this research was provided by the U.S. National Science

329 Foundation under grants OCE-1259398 and OCE-1756231. S. Zou is supported by the
330 U.S. National Science Foundation Grants OCE-1756361. Acknowledgement is extended
331 to C. Böning and A. Biastoch for providing FLAME output.

332 **Data Availability Statement**

333 OSNAP data used in this study are available online at <https://www.o-snap.org/observations/data>.
334 Datasets for this research are available in these in-text data citation references: Roemmich
335 and Gilson (2009), Johns et al. (2021-Under Review), and Elipot et al. (2016).

336 **References**

- 337 Belkin, I. M. (2004). Propagation of the “Great Salinity Anomaly” of the 1990s
338 around the northern North Atlantic. *Geophysical Research Letters*, *31*(8). doi:
339 10.1029/2003gl019334
- 340 Brambilla, E., & Talley, L. D. (2008). Subpolar Mode Water in the northeastern
341 Atlantic: 1. Averaged properties and mean circulation. *Journal of Geophysical*
342 *Research*, *113*(C4). doi: 10.1029/2006jc004062
- 343 Brambilla, E., Talley, L. D., & Robbins, P. E. (2008). Subpolar Mode Water in
344 the northeastern Atlantic: 2. Origin and transformation. *Journal of Geophysi-*
345 *cal Research*, *113*(C4). doi: 10.1029/2006jc004063
- 346 Dickson, B., Yashayaev, I., Meincke, J., Turrell, B., Dye, S., & Holfort, J. (2002).
347 Rapid freshening of the deep North Atlantic Ocean over the past four decades.
348 *Nature*, *416*(6883), 832–837. doi: 10.1038/416832a
- 349 Elipot, S., Lumpkin, R., Perez, R. C., Lilly, J. M., Early, J. J., & Sykulski, A. M.
350 (2016). A global surface drifter data set at hourly resolution. *Journal of*
351 *Geophysical Research: Oceans*, *121*(5), 2937–2966. doi: 10.1002/2016jc011716
- 352 Fogelqvist, E., Blindheim, J., Tanhua, T., Østerhus, S., Buch, E., & Rey, F. (2003).
353 Greenland–Scotland overflow studied by hydro-chemical multivariate analysis.
354 *Deep Sea Research Part I: Oceanographic Research Papers*, *50*(1), 73–102. doi:

- 355 10.1016/s0967-0637(02)00131-0
- 356 García-Ibáñez, M. I., Pardo, P. C., Carracedo, L. I., Mercier, H., Lherminier, P.,
 357 Ríos, A. F., & Pérez, F. F. (2015). Structure, transports and transformations
 358 of the water masses in the Atlantic Subpolar Gyre. *Progress in Oceanography*,
 359 *135*, 18–36. doi: 10.1016/j.pocean.2015.03.009
- 360 Gary, S. F., Susan Lozier, M., Böning, C. W., & Biastoch, A. (2011, September).
 361 Deciphering the pathways for the deep limb of the Meridional Overturning Cir-
 362 culation. *Deep Sea Research Part II: Topical Studies in Oceanography*, *58*(17),
 363 1781–1797. Retrieved 2021-05-16, from [https://www.sciencedirect.com/
 364 science/article/pii/S0967064511000221](https://www.sciencedirect.com/science/article/pii/S0967064511000221) doi: 10.1016/j.dsr2.2010.10.059
- 365 Hansen, B., & Østerhus, S. (2000). North Atlantic–Nordic Seas exchanges. *Progress*
 366 *in Oceanography*, *45*(2), 109–208. doi: 10.1016/s0079-6611(99)00052-x
- 367 Hansen, B., & Østerhus, S. (2007). Faroe Bank Channel overflow 1995–2005.
 368 *Progress in Oceanography*, *75*(4), 817–856. doi: 10.1016/j.pocean.2007.09.004
- 369 Holliday, N. P., Bersch, M., Berx, B., Chafik, L., Cunningham, S., Florindo-López,
 370 C., ... Yashayaev, I. (2020). Ocean circulation causes the largest freshening
 371 event for 120 years in eastern subpolar North Atlantic. *Nature Communica-*
 372 *tions*, *11*(1), 585. doi: 10.1038/s41467-020-14474-y
- 373 Houpert, L., Inall, M. E., Dumont, E., Gary, S., Johnson, C., Porter, M., ... Cun-
 374 ningham, S. A. (2018). Structure and Transport of the North Atlantic Current
 375 in the Eastern Subpolar Gyre From Sustained Glider Observations. *Journal of*
 376 *Geophysical Research: Oceans*, *123*(8), 6019–6038. doi: 10.1029/2018jc014162
- 377 Hátún, H., Sandø, A. B., Drange, H., Hansen, B., & Valdimarsson, H. (2005,
 378 September). Influence of the Atlantic Subpolar Gyre on the Thermohaline
 379 Circulation. *Science*, *309*(5742), 1841–1844. Retrieved 2021-05-10, from
 380 <https://science.sciencemag.org/content/309/5742/1841> (Publisher:
 381 American Association for the Advancement of Science Section: Report) doi:
 382 10.1126/science.1114777

- 383 Johns, W., Devana, M., Zou, S., & Houk, A. (2021-Under Review, July). Moored
384 observations of the Iceland-Scotland Overflow plume along the eastern flank of
385 the Reykjanes Ridge. *Journal of Geophysical Research: Oceans*.
- 386 Josey, S. A., Hirschi, J. J.-M., Sinha, B., Duchez, A., Grist, J. P., & Marsh, R.
387 (2018). The Recent Atlantic Cold Anomaly: Causes, Consequences, and
388 Related Phenomena. *Annual Review of Marine Science*, 10(1), 475–501. Re-
389 trieved 2021-05-10, from <https://doi.org/10.1146/annurev-marine-121916-063102>
390 (_eprint: <https://doi.org/10.1146/annurev-marine-121916-063102>)
391 doi: 10.1146/annurev-marine-121916-063102
- 392 Kanzow, T., & Zenk, W. (2014). Structure and transport of the Iceland Scotland
393 Overflow plume along the Reykjanes Ridge in the Iceland Basin. *Deep Sea Re-
394 search Part I: Oceanographic Research Papers*, 86, 82–93. doi: 10.1016/j.dsr
395 .2013.11.003
- 396 Lozier, M. S., Li, F., Bacon, S., Bahr, F., Bower, A. S., Cunningham, S. A., ... Zhao,
397 J. (2019). A sea change in our view of overturning in the subpolar North
398 Atlantic. *Science*, 363(6426), 516–521. doi: 10.1126/science.aau6592
- 399 McAdam, R., & Sebille, E. v. (2018). Surface Connectivity and Interocean Ex-
400 changes From Drifter-Based Transition Matrices. *Journal of geophysical re-
401 search. Oceans*, 123(1), 514–532. doi: 10.1002/2017jc013363
- 402 Roemmich, D., & Gilson, J. (2009). The 2004–2008 mean and annual cycle
403 of temperature, salinity, and steric height in the global ocean from the
404 Argo Program. *Progress in Oceanography*, 82(2), 81–100. doi: 10.1016/
405 j.pocean.2009.03.004
- 406 Sebille, E. v., Beal, L. M., & Johns, W. E. (2011). Advective Time Scales of Ag-
407 ulhas Leakage to the North Atlantic in Surface Drifter Observations and the
408 3D OFES Model. *Journal of Physical Oceanography*, 41(5), 1026–1034. doi:
409 10.1175/2011jpo4602.1
- 410 Ser-Giacomi, E., Rossi, V., López, C., & Hernández-García, E. (2015). Flow net-

- 411 works: A characterization of geophysical fluid transport. *Chaos: An Interdisci-*
412 *plinary Journal of Nonlinear Science*, 25(3), 036404. doi: 10.1063/1.4908231
- 413 Shao, Q., Zhao, J., Drinkwater, K. F., Wang, X., & Cao, Y. (2019). Internal
414 overflow in the Nordic Seas and the cold reservoir in the northern Nor-
415 wegian Basin. *Deep Sea Research Part I: Oceanographic Research Pa-*
416 *pers*, 148, 67–79. Retrieved from [https://ui.adsabs.harvard.edu/abs/](https://ui.adsabs.harvard.edu/abs/2019DSRI..148...67S/abstract)
417 [2019DSRI..148...67S/abstract](https://ui.adsabs.harvard.edu/abs/2019DSRI..148...67S/abstract) doi: 10.1016/j.dsr.2019.04.012
- 418 Zou, S., Lozier, S., Zenk, W., Bower, A., & Johns, W. (2017). Observed and
419 modeled pathways of the Iceland Scotland Overflow Water in the eastern
420 North Atlantic. *Progress in Oceanography*, 159, 211–222. doi: 10.1016/
421 [j.pocean.2017.10.003](https://doi.org/10.1016/j.pocean.2017.10.003)

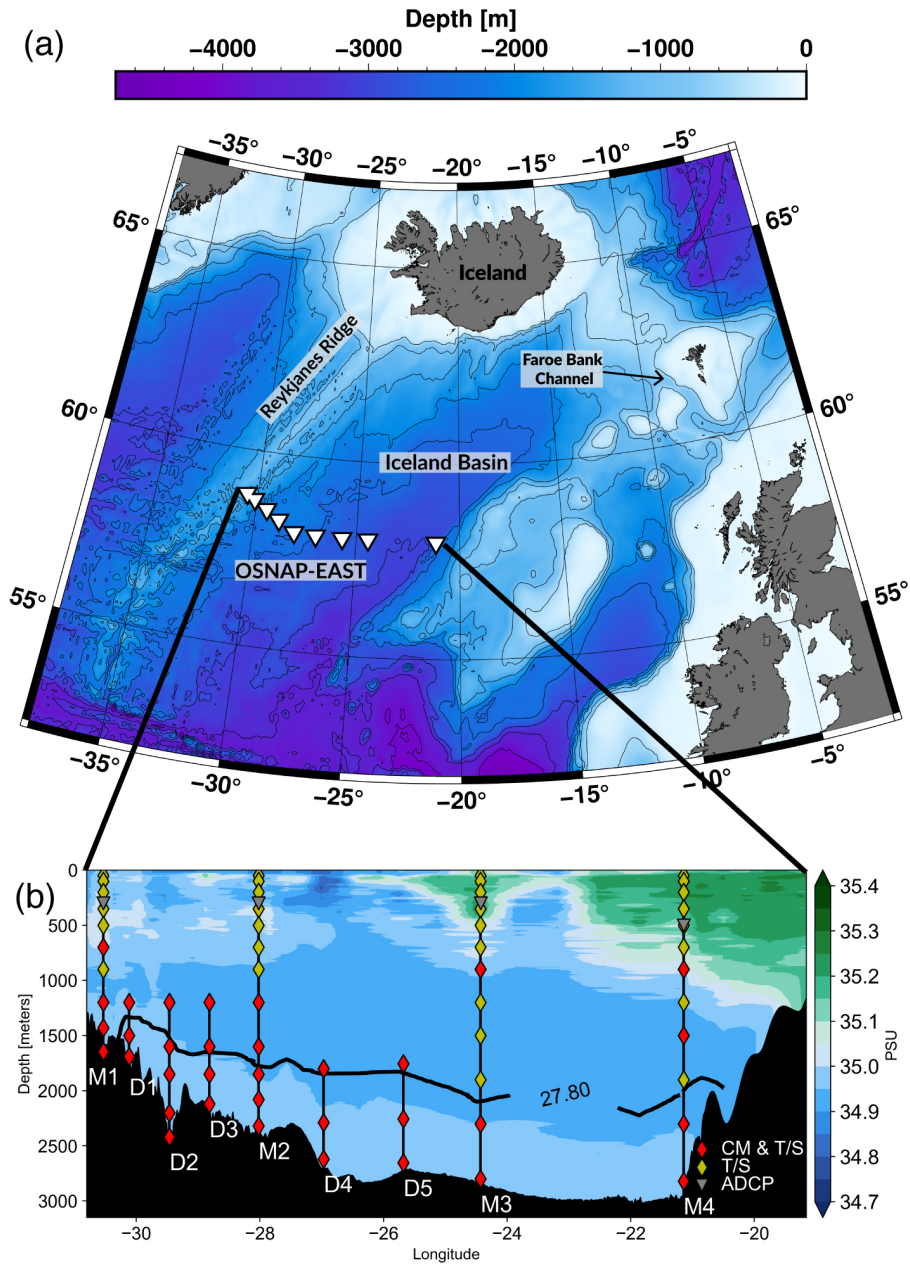


Figure 1. (a) Topographic map of the Iceland Basin and Iceland Faroe Ridge, with depth contours at 500 meter intervals. OSNAP mooring line indicated in red. (b) Configuration of the OSNAP-East mooring array with contours indicating salinity (PSU) from the 2018 OSNAP hydrographic section. Depths of temperature/salinity recorders, current meters, and ADCP's are indicated on each mooring.

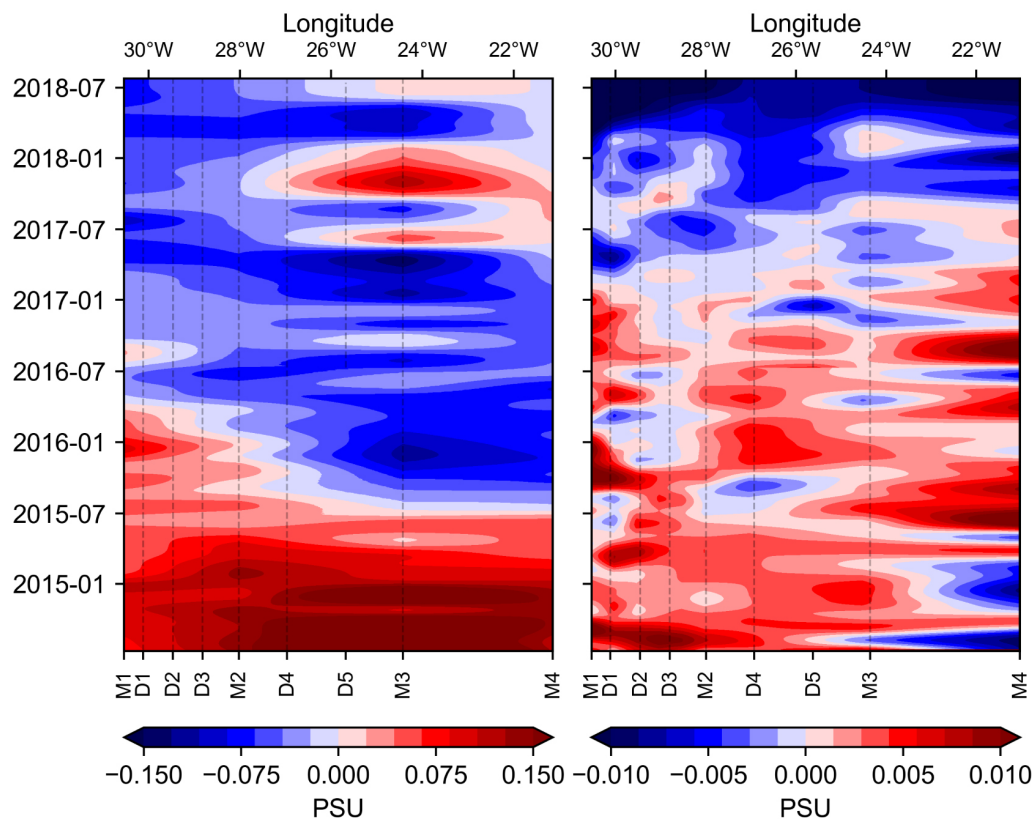


Figure 2. Hovmöllers of Mean OSNAP-EAST salinity anomalies (PSU) averaged over the upper 300 meters (left) and near-bottom (right). Data is at hourly resolution with a 60 day low-pass filter applied to both time series. Dashed lines indicate data coverage at each mooring. Note the different scales for the two plots, reflecting the larger range of salinity variability in the upper ocean. Anomalies are relative to the record mean (July 2014 - July 2018).

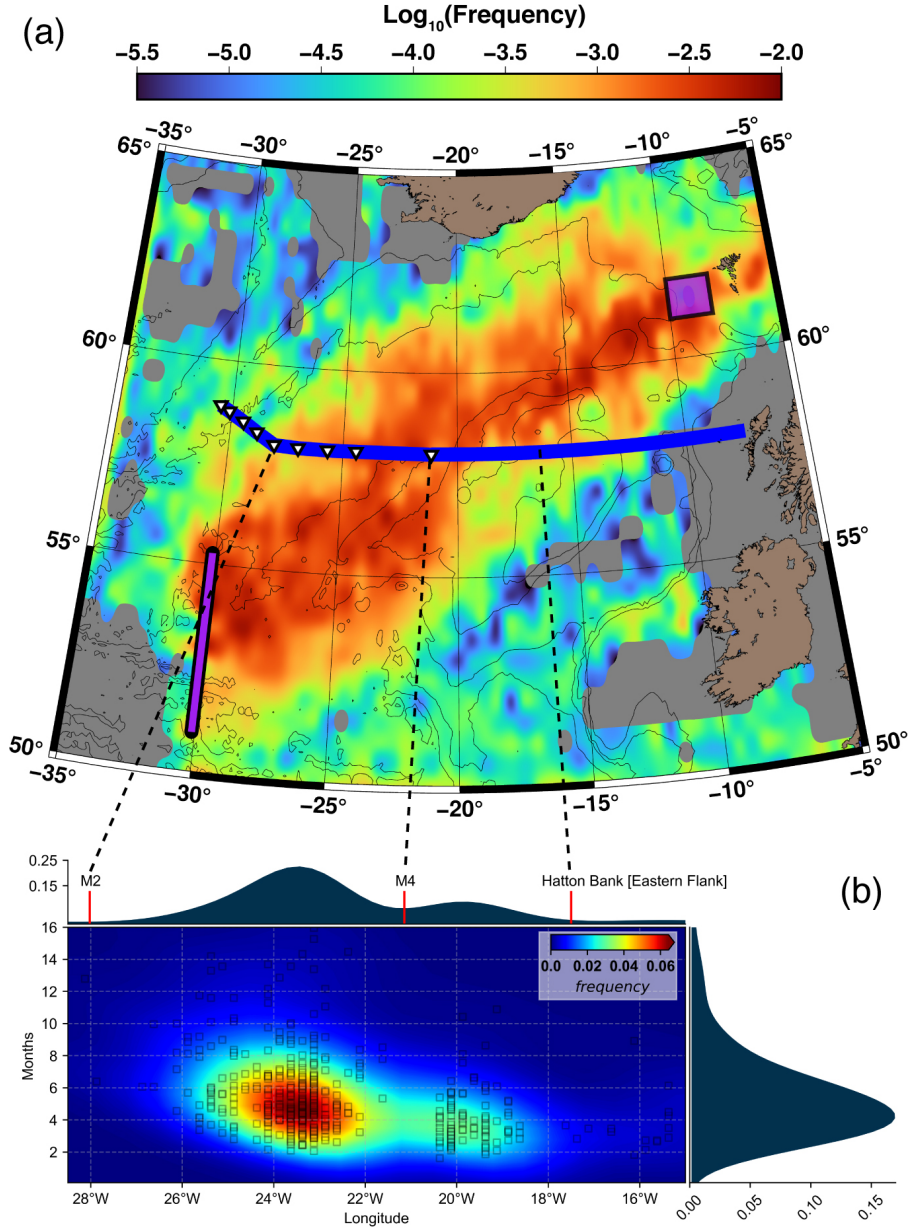


Figure 3. (a) The frequency distribution of simulated super trajectories released in the NAC (purple line) that reached the entrainment zone at Faroe Bank Channel (purple box). (b) The longitudinal distribution of trajectories crossing the The OSNAP line (blue line in a) vs. the advection time from the OSNAP line to the entrainment zone. The histograms along the top and right sides show the distributions of crossing longitudes and advection times to Faroe Bank Channel, respectively. OSNAP mooring locations are marked with triangles.

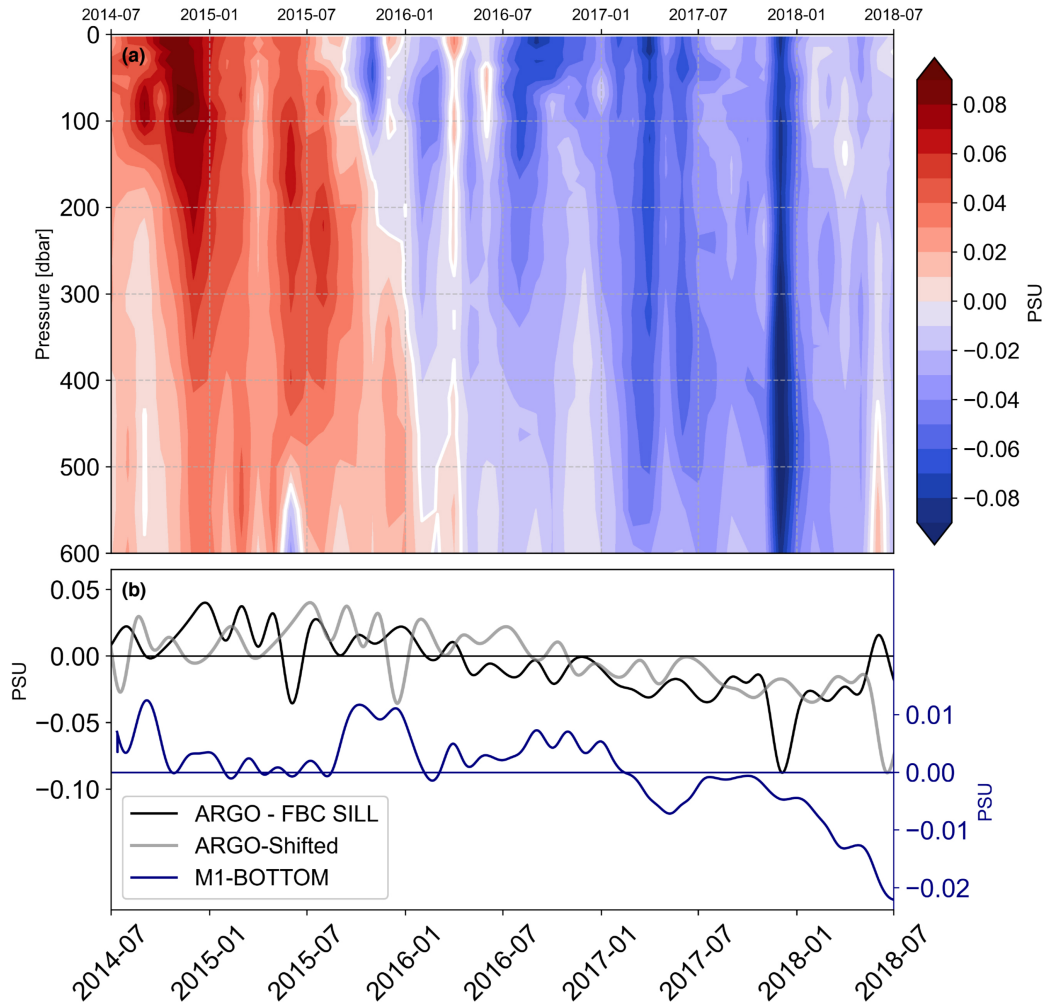


Figure 4. (a) Time series of salinity anomalies at the closest RGA grid point downstream of the FBC overflow sill (see Figure 1). Anomalies are relative to the July 2014-July 2018 mean, matching the OSNAP record’s coverage. The seasonal cycle has been removed to reduce influence from intense seasonal air-sea fluxes in the region. (b) RGA salinity anomaly time series at 600 meters depth (black-solid) and at the M1 near bottom salinity record (blue). The gray line is the 8-month shifted RGA time series. These time series are taken from the grid point closest to the FBC sill at 9.5° W, 61° N

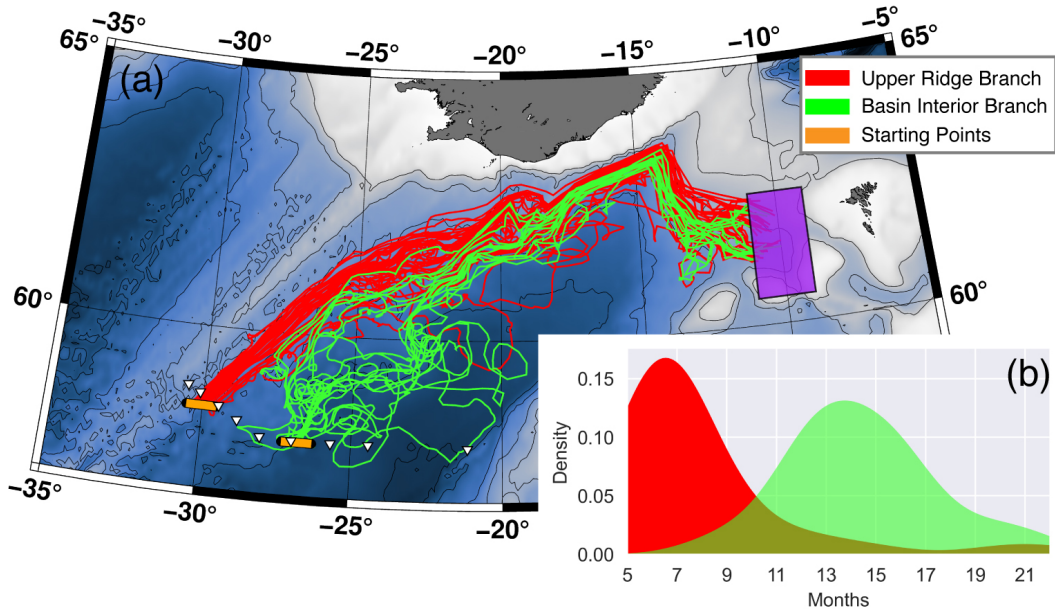


Figure 5. (a) FLAME model trajectories integrated backwards in time, released from the regions of moorings D1-D2 (red) and D4 (green). Orange bars indicate the range of longitudes where drifters were released. Trajectories are shown from their release sites back to the FBC sill. (b-inset) Histograms of advection times from FBC to the OSNAP line, with same color designation as the trajectories.